Triacetic acid lactone production using 2-pyrone synthase expressing Yarrowia lipolytica via targeted gene deletion

Matsuoka, Yuta ; Fujie, Naofumi ; Nakano, Mariko ; Koshiba, Ayumi ; Kondo, Akihiko ; Tanaka, Tsutomu

(Citation)
Journal of Bioscience and Bioengineering,136(4):320-326

(Issue Date)
2023-10

(Resource Type)
journal article

(Version)
Accepted Manuscript

(URL)
https://hdl.handle.net/20.500.14094/0100483436

Triacetic acid lactone production using 2-pyrone synthase expressing *Yarrowia lipolytica* via targeted gene deletion

Yuta Matsuoka[1], Naofumi Fujie[1], Mariko Nakano[1], Ayumi Koshiba[1], Akihiko Kondo[2,3], and Tsutomu Tanaka[1]*

[1]Department of Chemical Science and Engineering, Graduate School of Engineering, Kobe University, 1-1 Rokkodai, Nada, Kobe 657-8501, Japan

[2]Center for Sustainable Resource Science, RIKEN, 1-7-22 Suehiro-cho, Tsurumi-ku, Yokohama, Kanagawa 230-0045, Japan

[3]Graduate School of Science, Technology and Innovation, Kobe University, 1-1 Rokkodai, Nada, Kobe 657-8501, Japan

*Corresponding author: Tsutomu Tanaka

Email**:** tanaka@kitty.kobe-u.ac.jp

Tel/fax: +81-78-803-6202

Short title: TAL produced in *Y. lipolitica*

Key words: Triacetic acid lactone, *Yarrowia lipolytica*, metabolic engineering, CRIPSR-cas9, acetyl-CoA, malonyl-CoA, polyketide

Abstract

An environmentally sustainable world can be realized by using microorganisms to produce value-added materials from renewable biomass. Triacetic acid lactone (TAL) is a high-value-added compound that is used as a precursor of various organic compounds such as food additives and pharmaceuticals. In this study, we used metabolic engineering to produce TAL from glucose using an oleaginous yeast *Yarrowia lipolytica*. We first introduced TAL-producing gene 2-pyrone synthase into *Y. lipolytica*, which enabled TAL production. Next, we increased TAL production by engineering acetyl-CoA and malonyl-CoA biosynthesis pathways by redirecting carbon flux to glycolysis. Finally, we optimized the carbon and nitrogen ratios in the medium, culminating in the production of 4078 mg/L TAL. The strategy presented in this study had the potential to improve the titer and yield of polyketide biosynthesis.

Introduction

Oil refineries transform crude oil into various fuels for applications such as automobile engines and heating. However, these processing plants deplete fossil fuels and emit large amounts of carbon dioxide that accelerate global warming. Biorefineries use biomass, a renewable resource, as raw material and have therefore garnered attention as an environmentally friendly alternative to traditional refineries. By using microorganisms to synthesize chemicals, biorefineries not only generate value-added products but also will contribute to a more sustainable society (1, 2).

Triacetic acid lactone (4-hydroxy-6-methyl-2-pyrone) (TAL) is a natural compound of polyketide origin (3) and has a wide range of industrial applications; it serves as a precursor in the chemical synthesis of acetylacetone used in fuel additives, sorbic acid used in food additives, phloroglucinol used to synthesize heat-stable energy material 1,3,5-triamino-2,4,6-trinitrobenzene (TATB), and resorcinol used to formulate resins and adhesives (4, 5). Most commercially available TAL is obtained from gerbera (6) or chemically synthesized through a complicated organic synthesis involving petroleum-derived dehydroacetic acid (7). However, these expensive chemical methods generate hazardous by-products, deplete fossil fuels, and increase carbon dioxide emissions. Therefore, there is a need to develop technology for producing TALs from resource-based, metabolically engineered microorganisms.

TAL is synthesized by 2-pyrone synthase (2-PS) isolated from *Gerbera hybrida* (8), which is classified as a type III polyketide synthase. 2-PS catalyzes the synthesis of TAL from one acetyl-CoA and two malonyl-CoA molecules (9). Several studies have shown that 2-PS-expressing cells such as *E. coli* or *Saccharomyces cerevisiae* can produce TAL (10, 11). However, *E. coli* is an unlikely host for TAL production due to its toxic effects on cell growth (9). In contrast, *S. cerevisiae* can produce 1.6 g/L of TAL

with a yield of 0.16 g/g-glucose. This was accomplished by increasing cytosolic NADPH and eliminating the mitochondrial precursor transport pathway to enhance the flux to acetyl-CoA (12).

Yarrowia lipolytica is a non-conventional yeast that is phylogenetically distant from well-studied yeast species, such as *S. cerevisiae* (13). Its advantages include easy manipulation, rapid growth, and lack of pathogenicity, making it an excellent host for production of betulinic acid (14), resveratrol (15), and itaconic acid (16). *Y. lipolytica* can also reliably produce lipids and fatty acids due to its ability to generate acetyl-CoA and malonyl-CoA (17). Accordingly, a previous study achieved high titer of TAL in bioreactors by heterologous expression of 2-pyrone synthase for acetyl-CoA precursor formation (18).

In this study, we constructed a TAL-producing *Y. lipolytica* strain using metabolic engineering. After establishing the initial expression system, we engineered a metabolic pathway to enhance TAL biosynthesis by improving the precursors acetyl-CoA, malonyl-CoA, and NADPH via gene expression and gene disruption. To increase acetyl-CoA supply, we enhanced β-oxidation by overexpressing *pex10* and *por1*. For gene disruption, we targeted the TCA cycle by disrupting *cit1, ms1, ppc,* and *mae1*, which increased acetyl-CoA availability. Furthermore, we directed a carbon flux through the pentose phosphate pathway (PP pathway) to supplement NADPH. Then, by disrupting *dga1*, *lro1*, and *tgl3*, the fatty acid production pathway was modified to increase malonyl-CoA supply. Finally, TAL production was improved by optimizing the carbon and nitrogen sources in the culture medium.

Materials and methods

Strains and media

All strains used in this study are listed in Table 1. *Y. lipolytica* PO1f (ATCC MYA-2613) was used as the parental strain. The yeast strains were cultivated in YPD medium (BD Diagnostic Systems, Sparks, MD, USA) or YNB medium (Formedium, Norfolk, United Kingdom).

Construction of plasmids and homologous recombination (HR) donors

The plasmids used in this study are listed in Table S1, and the primers are listed in Table S2. The plasmid pCRISPRyl, expressing Cas9 and gRNA (19), was purchased from Addgene (Watertown, MA). A 20-base seed sequence together with the NGG PAM sequence (N20NGG) in the *Y. lipolytica* genome was selected using CHOPCHOP (https://chopchop.cbu.uib.no/). The HR donor sequences contained donor arms that were approximately 500 bp in length upstream and downstream of the Cas9 cutting site and the sites of the intended insertions. A Cas9 protein expression plasmid targeting the A08 gene was constructed using the KOD-Plus-mutagenesis Kit (TOYOBO, Co. Ltd. Osaka, Japan) according to the manufacturer's instructions. pCRISPRyl was used as a template with the primer pair fw-Cas9-A08-inv/rev-Cas9-A08-inv. The resulting plasmid was named pCRISPRyl_A08. Other plasmids for Cas9 targeting were constructed similarly and are summarized in Table S1.

A HR donor for 2-ps gene expression was constructed as follows: A DNA fragment was amplified with the primer pairs fw-2-ps-insert/rev-2-ps-insert using a codon-optimized 2-ps gene fragment (Invitrogen) as a template. The fragment was ligated into the *Asc*I and *Nhe*I sites of a plasmid pHR_A08_hrGFP (20). HR donor *pex10* gene expression was constructed as follows: The *pex10* gene fragment was amplified by PCR using primer pairs fw-AscI-pex10 and rev-NheI-por1 with the Po1f genomic DNA as a template. The fragment was ligated into the *Asc*I and *Nhe*I sites of pHR_A08_GFP. Using

the resultant plasmid as a template, the region encoding UAS1B8-TEF(136)promoter-pex10-CYCterminator was amplified with the primer pair fw-Avr2-d17 and rev-Spe1-d17. The upstream and downstream regions of the d17 gene were amplified with the primer pairs fw-BamHI-d17/rev-d17-2 and fw-d17-3/rev- BstBI-d17, respectively. These three amplified fragments were ligated into the *Bam*HI and *Bst*BI sites of pHR_A08_GFP using an In-Fusion HD cloning kit (Takara Bio, Japan). Other fragments were constructed similarly. In addition, the *d17, A08, c18, xyr11*, *xdh*, and *inte3* genes enable gene transfer and do not affect cell proliferation (21-23).

To construct HR donor DNA to disrupt the *cit1* gene, the upstream and downstream regions were amplified with the primer pairs fw-cit1-knock_out-1/rev-cit1-knock_out-2 and fw-cit1-knock_out-3/rev-cit1-knock_out-4, respectively. The two amplified fragments were conjugated using overlap extension PCR with the primer pair fw-cit1-knock_out-1/rev-cit1-knock_out-4. Other HR donor DNAs were constructed in the same way.

Transformation and culture conditions

All strains were constructed using the lithium acetate method (23) by co-transformation of 100 ng of the pCRISPRyl vector series with 500 ng of the respective HR donor DNA. Before the transformation, the cells were incubated overnight at 30 °C with shaking at 220 rpm in test tubes with 5 mL of YPD medium. Transformants were spread onto YNB plates supplemented with 125 mg/L uracil when needed. Transformants were screened using colony PCR using knock_out-1/knock_out-4 primer pairs and DNA sequencing. For TAL production, strains were pre-cultured in 5 mL of YPD medium for 48 hours at 30°C. This starter culture was used to inoculate 5 mL of YNB medium supplemented with 225 mg/L each of uracil and leucine at an initial O.D.600 of 0.3. The resulting culture was

agitated for 96 hours at 30°C at 220 rpm.

Analytical methods

Cell growth was evaluated by measuring the optical density at 600 nm with a UV mini-1240 spectrophotometer (Shimadzu Corporation, Kyoto, Japan). For TAL analysis, HPLC (Shimadzu Corporation) equipped with an MS II column (5 µm, 4.6 mm I.D. × 250 mm L; Nacalai Tesque) was used. HPLC profiles were obtained using a 254-nm UV-VIS detector. A two-component system was used: A) 0.2% phosphate buffer (mobile phase) and B) methanol. The gradient was initialized with a 70:30 mixture of A and B and shifted to a 50:50 mixture gradually from 4 minutes; the ratio was retained from 6 min to 14 min, and back to a 70:30 mixture at 16 minutes. The flow rate of the mobile phase was 1.0 mL/min, and the column remained at 40°C.

Results and discussion

Construction of the TAL production strain in *Y. lipolytica*

Fig. 1 depicts the TAL synthesis process. It is known that deleting *ku70* and *ku80*, the KU autoantigens required for the non-homologous end-joining pathway in *Y. lipolytica*, increases the relative rate of HR (24). However, the low efficiency of homology directed repair is also a limiting factor to genetic engineering in *Y. lipolytica*. Hence a dual cleavage strategy directed by CRIPSR/Cas9 system was applied to improve efficiency of genome engineering (25). Here, we deleted both *ku70* and *ku80* and introduced a codon-optimized *2-ps* gene into the *A08* locus using the CRISPR-Cas9 system. The resultant strain, TAL-1, produced 66.1 mg/L of TAL after 96 hours of cultivation in YNB+Leu+Ura medium containing 50 g/L glucose (Fig. 2). Furthermore, we created the TAL-2 strain by introducing an additional copy of the *2-ps* gene into the xyr11 locus of the TAL-1 strain.

Y. lipolytica has several kinds of xylose reductase related genes, but all of them except xyr2 gene has less enzymatic activities (26). The TAL-2 strain produced 425 mg/L of TAL, demonstrating a significant increase in production (Fig. 2).

Improvement of acetyl-CoA synthesis by enhanced β-oxidation

To improve TAL production, we overexpressed genes involved in the β-oxidation pathway. Fatty acid degradation in *Y. lipolytica* occurs through β-oxidation in peroxisomes, yielding acetyl-CoA and acyl-CoA. Subsequently, acetyl-CoA is used in the TCA cycle and glyoxylate circuits (27, 28). Our study aimed to increase acetyl-CoA synthesis during fatty acid degradation and use it for TAL production.

The target genes were *pex10* (YALI0C01023) and *por1* (YALI0D12628). The gene *pex10* encodes peroxisome biosynthesis factor 10 (29). In the case of *Pichia angusta*, expression of endogenous *pex10* increases the number of peroxisomes (30). The other *por1* gene encodes the primary oleate regulator 1, a transcriptional activator that broadly regulates fatty acid metabolism in *Y. lipolytica* (31, 32). In the case of *Aspergillus flavus,* expression of endogenous *por1* increased polyketide synthesis.

We constructed a TAL-3 strain overexpressing *pex10*, TAL-4 strain overexpressing *por1*, and TAL-5 strain overexpressing both *pex10* and *por1*. All strains increased production compared to TAL-1, especially the TAL-5 strain, which significantly increased production to 604 mg/L (Fig. 3A). A previous study reported that expression of *pex10* increased TAL production by 22% in *Y. lipolytica*, whereas expression of *por1* did not affect TAL production (18). Here, we found that the expression of two genes, *pex10* and *por1*, bolstered TAL production. These results suggest that expression of *pex10* and *por1* activates β-oxidation and increases acetyl-CoA synthesis, which increase TAL production. Further modification of β-oxidation may produce more

TAL.

Effects of improved Acetyl-CoA synthesis on the pyruvate bypass pathway modification

In *Y. lipolytica*, pyruvate is converted to acetaldehyde via pyruvate carboxylase (PDC)(YALI0D06930), then to acetate via acetaldehyde dehydrogenase (ALD)(YALI0D07942), and then converted to acetyl-CoA via acetyl-CoA synthetase (ACS)(YALI0F05962) (33). Acetyl-CoA is then converted to malonyl-CoA via acetyl-CoA carboxylase (ACC)(YALI0C11407) (34). A previous study reported that expression of genes in the pyruvate pathway significantly increases TAL production in *Y. lipolytica* (18). In this study, we sought to improve TAL production through expression of *pdc2, ald5, acs1,* and *acc1* to further increase acetyl-CoA synthesis. We constructed TAL-6 (TAL-5/Δ*inte3*::*acs1*), TAL-7 (TAL-5/Δ*inte3*::*pdc2*), TAL-8 (TAL-5/Δ*inte3*::*pdc2,*Δ*xdh*::*ald5*), TAL-9 (TAL-5/Δ*xyr11*::*acc1*), and TAL-10 (TAL-5/Δ*xyr11*::*acc1,*Δ*inte3*::*acs1*). However, all strains decreased TAL production (Fig. 3B). Previous research suggested that multiple copies of each gene must be included to enhance TAL production (18). Therefore, we pursued a different approach.

Improvement of acetyl-CoA synthesis by gene disruption -related TCA cycle

We reduced the flux to the TCA cycle to increase acetyl-CoA synthesis and therefore TAL production by focusing on *cit1*-encoding citrate synthase (YALI0E00638), *mae1* encoding malate dehydrogenase (YALI0E18634), *ms1*-encoding malate synthase (YALI0D19140), and *ppc*-encoding phosphoenolpyruvate carboxylase (YALI0C16995). These genes in the TAL-1 strain were disrupted, and TAL production of the resultant strains was evaluated (Fig. 4A). The TAL-11 strain with *cit1* disruption successfully

224 increased production to 177 mg/L compared to TAL-1 (66 mg/L; Fig. 2). Despite the role
225 of *cit1* in the flow of carbon to the TCA cycle, its destruction did not affect cell growth,
226 possibly due to the presence of *cit2* (YALI0E02684). The gene *cit2* encodes a 2-
227 methylcitrate synthase involved in the formation of 2-methylcitrate from the condensation
228 of propionyl-CoA and oxaloacetic acid in the 2-methylcitrate cycle (35). CIT2 accepts
229 acetyl-CoA as a substrate, allowing the TCA cycle to function normally. Growth was not
230 affected by the disruption of *cit1*. Alternatively, the deletion of other genes involved in
231 the TCA cycle, such as *pyc*, *mae1*, *ppc*, and *mae1* decreased TAL production (less than
232 50 mg/L, data not shown). To further investigate the factors affecting TAL biosynthesis,
233 we constructed TAL-1-based-double-deletion-mutants, including *Δmae1Δms1*,
234 *Δmae1Δpyc*, *Δms1Δpyc*, *Δms1Δppc*, and *ΔpycΔppc*. Unfortunately, all strains reduced
235 TAL production to less than 50 mg/L (data not shown). We also constructed triple-
236 deletion-mutants: TAL-12 (TAL-1/*Δcit1Δmae1Δms1*), TAL-13 (TAL-
237 1/*Δcit1Δmae1Δppc*), and TAL-14 (TAL-1/*Δcit1Δms1Δppc*). These strains performed
238 similarly to the TAL-11 strain (Fig. 4A), suggesting that *cit1* disruption is an effective
239 approach for increasing TAL production. The acetyl-CoA concentration of TAL-13 was
240 1.3-fold higher compared to that of TAL-1 (data not shown). In contrast, AMP deaminase
241 expression barely affects TAL production (18). Overall, *cit1* disruption enhances TAL
242 production without inhibiting cell growth (Fig. 4A).
243
244 **Rewiring carbon flux to the PP pathway or EM pathway by gene disruption**
245 NADPH is a rate-limiting metabolite for fatty acid and lipid synthesis initiated by
246 malonyl-CoA in *Y. lipolytica* (36, 37). We sought to improve TAL production by
247 disrupting specific genes to upregulate NADPH synthesis. To channel more carbon to the
248 PP pathway and increase NADPH production, we focused on the *pgi*-encoding glucose-

6-phosphate isomerase (YALI0F07711). Disruption of the *pgi* gene can increase carbon flow to the PP pathway (38), since *pgi* is the gene responsible for the first reaction in glycolysis (39). We constructed a TAL-15 strain (TAL-1/*Δpgi*); however, TAL production was only 67 mg/L (Fig. 4B), which was almost the same as that of TAL-1(Fig. 2). Although the PP pathway is the main source of NADPH for lipid production (36), increasing the supply of cofactor NADPH did not significantly increase terpenoid production (40). Similarly, our results suggest a sufficient supply of NADPH in TAL-1 and TAL-15 strains.

Next, we focused on the *fbp1*-encoding fructose-1,6-bisphosphatase I (YALI0A15972), to redirect carbon flux to the Embden-Meyerhof pathway. Fructose-1,6-bisphosphatase 1, a gluconeogenesis regulatory enzyme, catalyzes the hydrolysis of fructose 1,6-bisphosphate to fructose 6-phosphate. We constructed a TAL-16 strain (TAL-1/*Δfbp1*), resulting in 115 mg/L of TAL production and improved cell growth (Fig. 4B). The double mutant, TAL-17 (TAL-1/*Δfbp1Δpgi*), decreased TAL production. The cell growth of TAL-16 was improved, and slightly decreased that of TAL-17 (Fig. 4B). It suggests the disruption of *fbp1* may enhance carbon flux into PP pathway and improve NADPH availability. These results suggest that rewiring carbon flux via the EM pathway is more effective for TAL production than manipulating the PP pathway.

Improving malonyl-CoA synthesis by modifying fatty acid biosynthesis pathways

Malonyl-CoA is a crucial precursor for TAL synthesis and fatty acid synthesis. Cerulenin, an antibiotic inhibitor of fatty acid synthesis, can increase the accumulation of malonyl-CoA (41). Although the addition of cerulenin in TAL-1 cultivation increased TAL production up to 901 mg/L (Fig. 5A), the high cost of cerulenin renders it impractical for bioproduction. Therefore, we aimed to improve TAL production by disrupting genes

related to the fatty acid biosynthesis pathway.

We targeted the genes *dga1*-encoding diacylglycerol O-acyltransferase I (YALI0D07986), *lro1*-encoding phospholipid:diacylglycerol acyltransferase (YALI0E16797), and *tgl3*-encoding lysophosphatidylethanolamine acyltransferase (YALI0D17534). In *Rhodotorula toruloides,* disruption of *dga1* and *lro1* increased TAL production by 11% and 19%, respectively (42). We disrupted these genes in the TAL-1 strain, constructing TAL-18 (TAL-1/*Δdga1*), TAL-19 (TAL-1/*Δlro1*), and TAL-20 (TAL-1/*Δtgl3*). All three strains increased TAL production to over 100 mg/L (Fig. 5B), superior to TAL-1 (Fig. 2). The cell growth of TAL-18, TAL-19 and TAL-20 was improved, (Fig. 5B), suggesting rewiring carbon flux from fatty acid synthesis to cell growth. Thus, the availability of malonyl-CoA is an important factor for TAL synthesis. We then constructed double- and triple-disruption mutants, TAL-21 (TAL-1/*Δdga1Δtgl3*) and TAL-22 (TAL-1/*Δdga1Δtgl3Δlro1*), respectively. However, both strains did not improve TAL production (Fig. 5B), possibly due to the metabolic burden of excessive gene disruption.

increased carbon/nitrogen ratio in culture medium increases TAL production

It is widely accepted that increasing the C/N ratio (carbon source/nitrogen source) of the culture medium suppresses fungal growth (43). We constructed a TAL-23 strain (TAL-2/Δ*d17*::*pex10*, Δ*c18*::*por1*) that produced 1720 mg/L of TAL (Fig. 6). Notably, the combination of 2-copies of 2-ps gene introduction (Fig. 2) and expression of both *pex10* and *por1* (Fig. 3A) improved TAL production. When TAL-23 was cultivated in a medium with a high C/N ratio, TAL production reached 4078 mg/L (Fig. 6). As previously reported, cell growth slightly decreased with increasing C/N ratio (43). Our findings highlight the importance of optimizing the C/N ratio of the culture medium and the balance between TAL and lipid biosynthesis.

In conclusion, we produced TAL from glucose in *Y. lipolytica*. We focused on the precursors acetyl-CoA, malonyl-CoA, and NADPH to improve TAL production by gene expression and gene disruption. In addition, optimizing the carbon and nitrogen ratio in the culture medium increased TAL production to 4078 mg/L. In a previous study, production was increased to 4 g/L by overexpressing genes related to TAL production and optimizing the C/N ratio. In this study, we succeeded in similarly improving TAL production to same levels using a gene disruption approach. Ultimately, this study demonstrated the suitability of an oleaginous yeast as a host to produce TAL and possibly other polyketides.

Conflict of interest

The authors declare no competing interests.

Acknowledgments

This work was supported by the Japan Society for the Promotion of Science (JSPS) Grant-in-Aid for Scientific Research (B) (grant number 22H01880) and (A) (Grant Number 20H00321). Y.M. and T.T conceived and designed the research. Y.M. A. Koshiba and M.N. conducted the experiments. A.K contributed new reagents. Y.M. and T.T analyzed data and wrote the manuscript. All authors read and approved the manuscript.

References

1. **Kamm, B., Schönicke, P. and Hille, Ch**.: Green biorefinery – industrial implementation, Food Chem., **197**, 1341–1345 (2016).

2. **Octave, S. and Thomas, D**.: Biorefinery: Toward an industrial metabolism, Biochimie, **91**, 659–664 (2009).

3. **Bentley, R. and Zwitkowits, P.M**.: Biosynthesis of tropolones in *Penicillium stipitatum*. 8. The utilization of polyketide lactones for tropolone formation, J. Am. Chem. Soc., **89**, 681–685 (1967).

4. **Chia, M., Schwartz, T.J., Shanks, B.H. and Dumesic, J.A.**: Triacetic acid lactone as a potential biorenewable platform chemical, Green Chem., 14, 1850–1853 (2012).

5. **Hansen, C. A. and Frost, J. W**.: Deoxygenation of polyhydroxybenzenes: an alternative strategy for the benzene–free synthesis of aromatic chemicals, J. Am. Chem. Soc., **124**, 5926–5927 (2002).

6. **Yrjönen, T., Vuorela, P., Klika, K.D, Pihlaja, K., Teeri, T.H. and Vuorela, H**.: Application of centrifugal force to the extraction and separation of parasorboside and gerberin from *Gerbera hybrida*, Phytochem. Anal., **13**, 349–353 (2002).

7. **Weissermel, K**.: Industrial organic chemistry, John Wiley & Sons, (2008)

8. **Eckermann, S., Schröder, G., Schmidt, J. Strack, D., Edrada, R.A., Helariutta, Y., Elomaa, P., Kotilainen, M., Kilpeläinen, I., Proksch, P., Teeri, T.H. and Schröder, J**.: New pathway to polyketides in plants, Nature, **396**, 387–390 (1998).

9. **Xie, D., Shao, Z., Achkar, J., Zha, W., Frost, J.W. and Zhao, H**.: Microbial synthesis of triacetic acid lactone, Biotechnol. Bioeng., **93**, 727–736 (2006).

10. **Tang, S.Y., Qian, S., Akinterinwa, O., Frei, C.S., Gredell, J,A. and Cirino, P.C**.: Screening for enhanced triacetic acid lactone production by recombinant *Escherichia coli* expressing a designed triacetic acid lactone reporter, J. Am. Chem. Soc. **135**, 10099–10103 (2013).

11. **Cardenas, J. and Da Silva, N.A**.: Metabolic engineering of *Saccharomyces cerevisiae* for the production of triacetic acid lactone, Metab. Eng., **25**, 194–203 (2014).

12. **Cardenas, J., and Da Silva, N.A**.: Engineering cofactor and transport mechanisms in *Saccharomyces cerevisiae* for enhanced acetyl–CoA and polyketide biosynthesis, Metab. Eng., **36**, 80–89 (2016).

13. **Barth, G. and Gaillardin, C**.: Yarrowia lipolytica, pp. 313–388, in: Wolf, K. (Ed.), Nonconventional yeasts in biotechnology: A Handbook, Springer–Verlag (2013),

14. **Jin, C.C., Zhang, J.L., Song, H. and Cao, Y.X**.: Boosting the biosynthesis of betulinic acid and related triterpenoids in *Yarrowia lipolytica* via multimodular metabolic engineering, Microb. Cell Fact., **18**, 77 (2019).

15. **Sáez–Sáez, J., Wang, G., Marella, E.R., Sudarsan, S., Cernuda Pastor, M. and Borodina, I.**: Engineering the oleaginous yeast *Yarrowia lipolytica* for high–level resveratrol production, Metab. Eng., **62**, 51–61 (2020).

16. **Blazeck, J., Hill, A., Jamoussi, M., Pan, A., Miller, J. and Alper, H.S**.: Metabolic engineering of *Yarrowia lipolytica* for itaconic acid production, Metab. Eng., **32**, 66–73 (2015).

17. **Levering, J., Broddrick, J. and Zengler, K**.: Engineering of oleaginous organisms for lipid production, Curr. Opin. Biotechnol., **236**, 32–39 (2015).

18. **Markham, K.A., Palmer, C.M., Chwatko, M., Wagner, J.M., Murray, C., Vazquez, S., Swaminathan, A., Chakravarty, I., Lynd, N.A. and Alper, H.S**.: Rewiring *Yarrowia lipolytica* toward triacetic acid lactone for materials generation, Proc. Natl. Acad. Sci. U.S.A., **115**, 2096–2101(2018).

19. **Schwartz, C.M., Hussain, M.S., Blenner, M. and Wheeldon, I.**: Synthetic RNA polymerase III promoters facilitate high–efficiency CRISPR–Cas9–mediated genome editing in *Yarrowia lipolytica*, ACS Synth. Biol., **5**, 356–359 (2016).

20. **Schwartz, C., Shabbir–Hussain, M., Frogue, K., Blenner, M. and Wheeldon, I.**: Standardized markerless gene integration for pathway engineering in *Yarrowia*

lipolytica, ACS Synth. Biol., **6**, 402–409 (2017).

21. **Rodriguez, G.M., Hussain, M.S., Gambill, L., Gao, D., Yaguchi, A. and Blenner, M.**: Engineering xylose utilization in *Yarrowia lipolytica* by understanding its cryptic xylose pathway, Biotechnol. Biofuels., **9**, 149 (2016).

22. **Lee, J.W., Yook, S., Koh, H., Rao, C.V. and Jin, Y.S**.: Engineering xylose metabolism in yeasts to produce biofuels and chemicals, Curr. Opin. Biotechnol., **67**, 15–25 (2021).

23. **Gietz, R.D. and Schiestl, R.H**.: High–efficiency yeast transformation using the LiAc/SS carrier DNA/PEG method, Nat. Protoc., **2**, 31–34 (2007).

24. **Schwartz, C., Frogue, K., Ramesh, A., Misa, J. and Wheeldon, I**.: CRISPRi repression of nonhomologous end–joining for enhanced genome engineering via homologous recombination in *Yarrowia lipolytica*, Biotechnol. Bioeng., **114**, 2896–2906 (2017).

25. **Bae, S.J., Park, B.G., Kim, B.G. and Hahn, J.S**.: Multiplex gene disruption by targeted base editing of *Yarrowia lipolytica* genome using cytidine deaminase combined with the CRISPR/Cas9 system, Biotechnol. J., **15**, e1900238, (2020).

26. **Niehus, X., Crutz-Le Coq, A.M., Sandoval, G., Nicaud, J.M. and Ledesma-Amaro R**.: Engineering *Yarrowia lipolytic*a to enhance lipid production from lignocellulosic materials, Biotechnol. Biofuels, **11**, 11. (2018).

27. **Beopoulos, A., Chardot, T. and Nicaud, J.M.**: *Yarrowia lipolytica*: A model and a tool to understand the mechanisms implicated in lipid accumulation, Biochimie, **91**, 692–696 (2009).

28. **Zeng, S.Y., Liu, H.H., Shi, T.Q., Song, P., Ren, L.J., Huang, H. and Ji, X.J.**: Recent advances in metabolic engineering of *Yarrowia lipolytica* for lipid overproduction, Eur. J. Lipid. Sci. Technol., **120**, 1700352 (2018).

399 29. **Sumita, T., Iida, T., Hirata, A., Horiuchi, H., Takagi, M. and Ohta, A.**:
400 Peroxisome deficiency represses the expression of n–alkane–inducible YlALK1
401 encoding cytochrome P450ALK1 in *Yarrowia lipolytica*. FEMS Microbiol. Lett., 214,
402 31–38 (2002).
403 30. **Tan, X., Waterham, H.R., Veenhuis, M. and Cregg, J.M.**: The Hansenula
404 polymorpha PER8 gene encodes a novel peroxisomal integral membrane protein
405 involved in proliferation, J. Cell Biol., **128**, 307–319 (1995).
406 31. **Luo, X., Affeldt, K.J. and Keller, N.P**.: Characterization of the far transcription
407 factor family in *Aspergillus flavus*, G3 (Bethesda), **6**, 3269–3281 (2016).
408 32. **Poopanitpan, N., Kobayashi, S., Fukuda, R., Horiuchi, H. and Ohta, A**.: An
409 ortholog of farA of *Aspergillus nidulans* is implicated in the transcriptional activation of
410 genes involved in fatty acid utilization in the yeast *Yarrowia lipolytica*, Biochem.
411 Biophys. Res. Commun., **402**, 731–735 (2010).
412 33. **Flores, C.L., Rodríguez, C., Petit, T. and Gancedo, C**.: Carbohydrate and energy–
413 yielding metabolism in non–conventional yeasts, FEMS Microbiol. Rev., **24**, 507–529
414 (2000).
415 34. **Liu, H., Marsafari, M., Deng, L. and Xu, P**.: Understanding lipogenesis by
416 dynamically profiling transcriptional activity of lipogenic promoters in *Yarrowia*
417 *lipolytica*, Appl. Microbiol. Biotechnol., **103**, 3167–3179 (2019).
418 35. **Papanikolaou, S., Beopoulos, A., Koletti, A., Thevenieau, F., Koutinas, A.A.,**
419 **Nicaud, J.M. and Aggelis, G**.: Importance of the methyl–citrate cycle on glycerol
420 metabolism in the yeast *Yarrowia lipolytica*, J. Biotechnol., **168**, 303–314 (2013).
421 36. **Wasylenko, T.M., Ahn, W.S. and Stephanopoulos, G.**: The oxidative pentose
422 phosphate pathway is the primary source of NADPH for lipid overproduction from
423 glucose in *Yarrowia lipolytica*, Metab. Eng., **30**, 27–39 (2015).

37. **Qiao, K., Wasylenko, T.M., Zhou, K., Xu, P. and Stephanopoulos, G**.: Lipid production in *Yarrowia lipolytica* is maximized by engineering cytosolic redox metabolism, Nat. Biotechnol., **35**, 173–177 (2017).

38. **Lin, Z., Xu, Z., Li, Y., Wang, Z., Chen, T. and Zhao, X**.: Metabolic engineering of *Escherichia coli* for the production of riboflavin, Microb. Cell Fact., **13**, 104 (2014).

39. **Satowa, D., Fujiwara, R., Uchio, S., Nakano, M., Otomo, C., Hirata, Y., Matsumoto, T., Noda, S., Tanaka, T., and Kondo, A**.: Metabolic engineering of E. coli for improving mevalonate production to promote NADPH regeneration and enhance acetyl–CoA supply, Biotechnol. Bioeng., 117, 2153–2164 (2020).

40. **Li, Z.J., Wang, Y.Z., Wang, L.R., Shi, T.Q., Sun, X.M. and Huang, H**.: Advanced strategies for the synthesis of terpenoids in *Yarrowia lipolytica*, J. Agric. Food. Chem., 69, 2367–2381 (2021).

41. **Davis, M.S., Solbiati, J. and Cronan, J.E. Jr.**: Overproduction of acetyl–CoA carboxylase activity increases the rate of fatty acid biosynthesis in *Escherichia coli*, J. Biol. Chem., **275**, 28593–28598 (2000).

42. **Cao, M., Tran, V.G., Qin, J., Olson, A., Mishra, S., Schultz, J.C., Huang, C., Xie, D. and Zhao, H**.: Metabolic engineering of oleaginous yeast *Rhodotorula toruloides* for overproduction of triacetic acid lactone, Biotechnol. Bioeng., **119**, 2529–2540 (2022).

43. **Ma, Y., Liu, N., Greisen, P., Li, J., Qiao, K., Huang, S. and Stephanopoulos, G**.: Removal of lycopene substrate inhibition enables high carotenoid productivity in *Yarrowia lipolytica*, Nat. Commun., **13**, 572 (2022).

Figure Legends

FIG. 1 Metabolic engineering of TAL-producing *Y. lipolytica*. Red indicates genes

449 involved in TAL synthesis and expression of the *pex10, por1, pdc2, ald5, acs1*, and
450 *acc1* genes. The blue X indicates disruption of the *cit1*, *mae1*, *ms1, ppc, pgi, fbp1, dga1,*
451 *lro1*, and *tgl3* genes. 2-PS, 2-pyrone synthase from *Gerbera hybrida*; pex10, peroxin-
452 10; por1, primary oleate regulator I; pdc2, pyruvate carboxylase; ald5, acetaldehyde
453 dehydrogenase; acs1, acetyl-CoA synthetase; acc1, acetyl-CoA carboxylase; cit1, citrate
454 synthase; mae1, malate dehydrogenase; ms1, malate synthethase; ppc,
455 phosphoenolpyruvate carboxylase; *pgi*, glucose-6-phosphate isomerase; fbp1, fructose-
456 1,6-bisphosphatase I; dga1, diacylglycerol O-acyltransferase I; lro1,
457 phospholipid:diacylglycerol acyltransferase; tgl3, lysophosphatidylethanolamine
458 acyltransferase.
459
460 **FIG. 2**. TAL production after 96 hours of cultivation in YNB+Ura+Leu medium
461 containing 50 g/L glucose using TAL-1 and TAL-2 strains. Blue bars indicate TAL
462 concentration, and yellow bars show cell growth. Data are shown as the means and
463 standard deviations of three independent experiments.
464
465 **FIG. 3**. Improving TAL production through A) the β-oxidation pathway and B) the
466 pyruvate bypass pathway. Blue bars indicate TAL concentration, and yellow bars show
467 cell growth. TAL production after 96 hours of cultivation in YNB+Ura+Leu medium
468 containing 50 g/L glucose. Data are shown as the means and standard deviations of
469 three independent experiments.
470
471 **FIG. 4**. Improving TAL production by modifying the A) TCA cycle and B) EMP
472 pathway. Blue bars indicate TAL concentration, and yellow bars show cell growth. TAL
473 production after 96 hours of cultivation in YNB+Ura+Leu medium containing 50 g/L

glucose. Data are shown as the means and standard deviations of three independent experiments.

FIG. 5. A) TAL production after 96 hours of cultivation in YNB+Ura+Leu medium containing 50 g/L glucose in the presence of 5 mg/L of cerulenin. Blue bars indicate TAL concentration, and yellow bars show cell growth. Data are shown as the means and standard deviations of three independent experiments. B) Improving TAL production by modifying the fatty acid synthesis pathway. TAL production after 96 hours of cultivation in YNB+Ura+Leu medium containing 50 g/L glucose. Blue bars indicate TAL concentration, and yellow bars show cell growth. Data are shown as the means and standard deviations of three independent experiments.

FIG. 6. TAL production after 120 hours of cultivation in YNB+Ura+Leu medium containing 50 g/L glucose, $Y_{10}P_{20}D_{50}$ medium (10 g/L yeast exact, 20 g/L peptone), $Y_{10}P_{10}D_{50}$ medium (10 g/L yeast exact, 10 g/L peptone), $Y_5P_{10}D_{50}$ medium (5 g/L yeast exact, 10 g/L peptone) containing 50 g/L glucose using TAL-23 strains. Blue bars indicated TAL concentration, and yellow bars show cell growth. Data are shown as the means and standard deviations of three independent experiments.

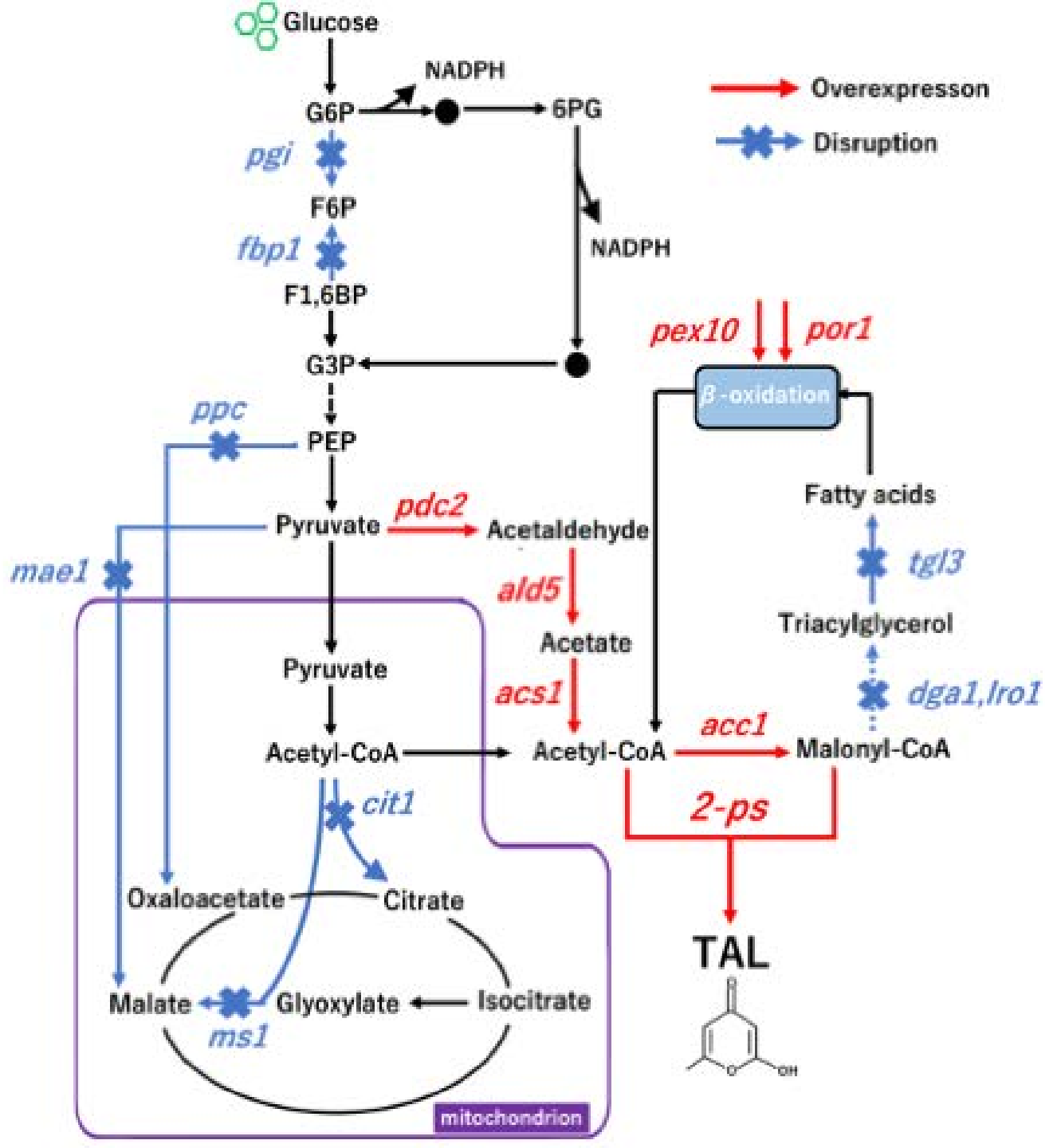
Glucose
NADPH
G6P
6PG
Overexpresson
Disruption
pgi
F6P
fbp1
NADPH
F1,6BP
pex10
por1
G3P
β-oxidation
ppc
PEP
Fatty acids
pdc2
Pyruvate
Acetaldehyde
tgl3
mae1
ald5
Triacylglycerol
Acetate
Pyruvate
acs1
dga1,lro1
acc1
Acetyl-CoA
Acetyl-CoA
Malonyl-CoA
cit1
2-ps
Oxaloacetate
Citrate
TAL
Malate
Glyoxylate
Isocitrate
ms1
mitochondrion

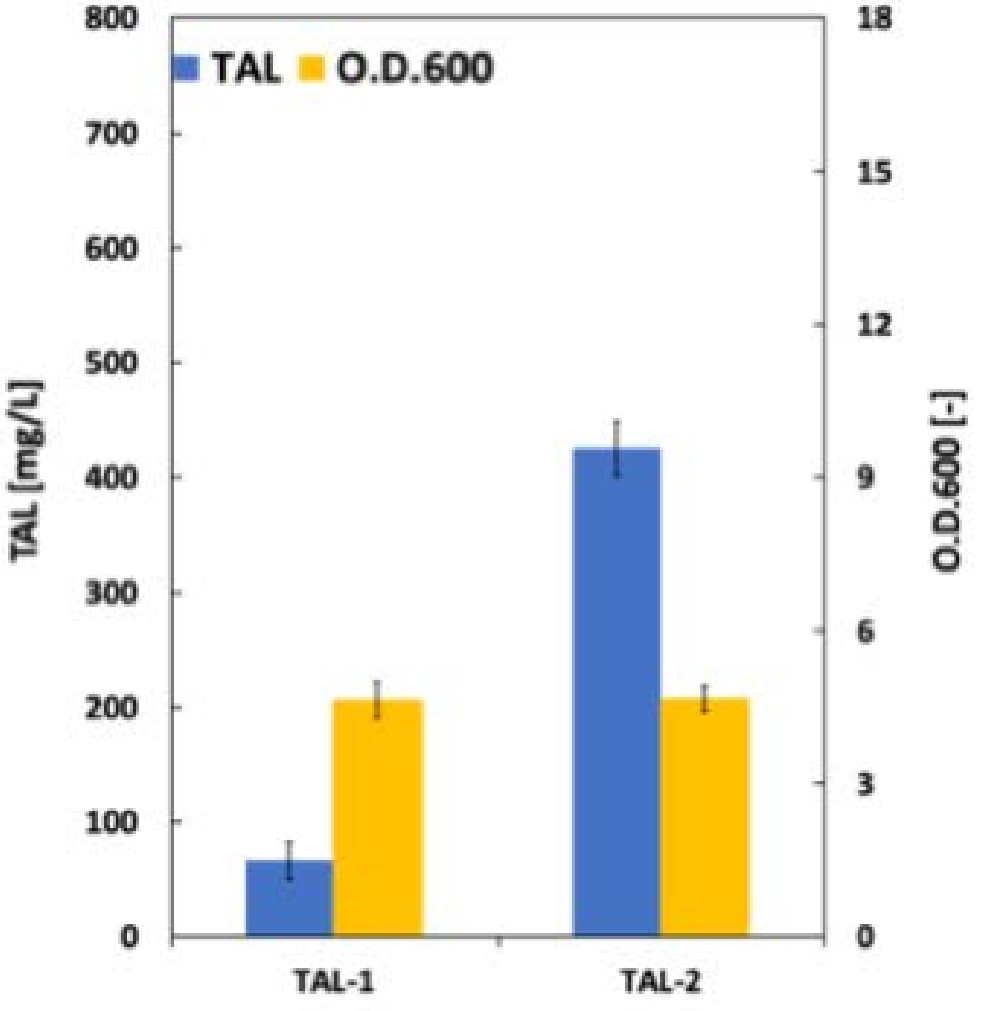
TAL
O.D.600
800
700
600
500
400
300
200
100
0
18
15
12
9
6
3
0
TAL [mg/L]
O.D.600 [-]
TAL-1
TAL-2

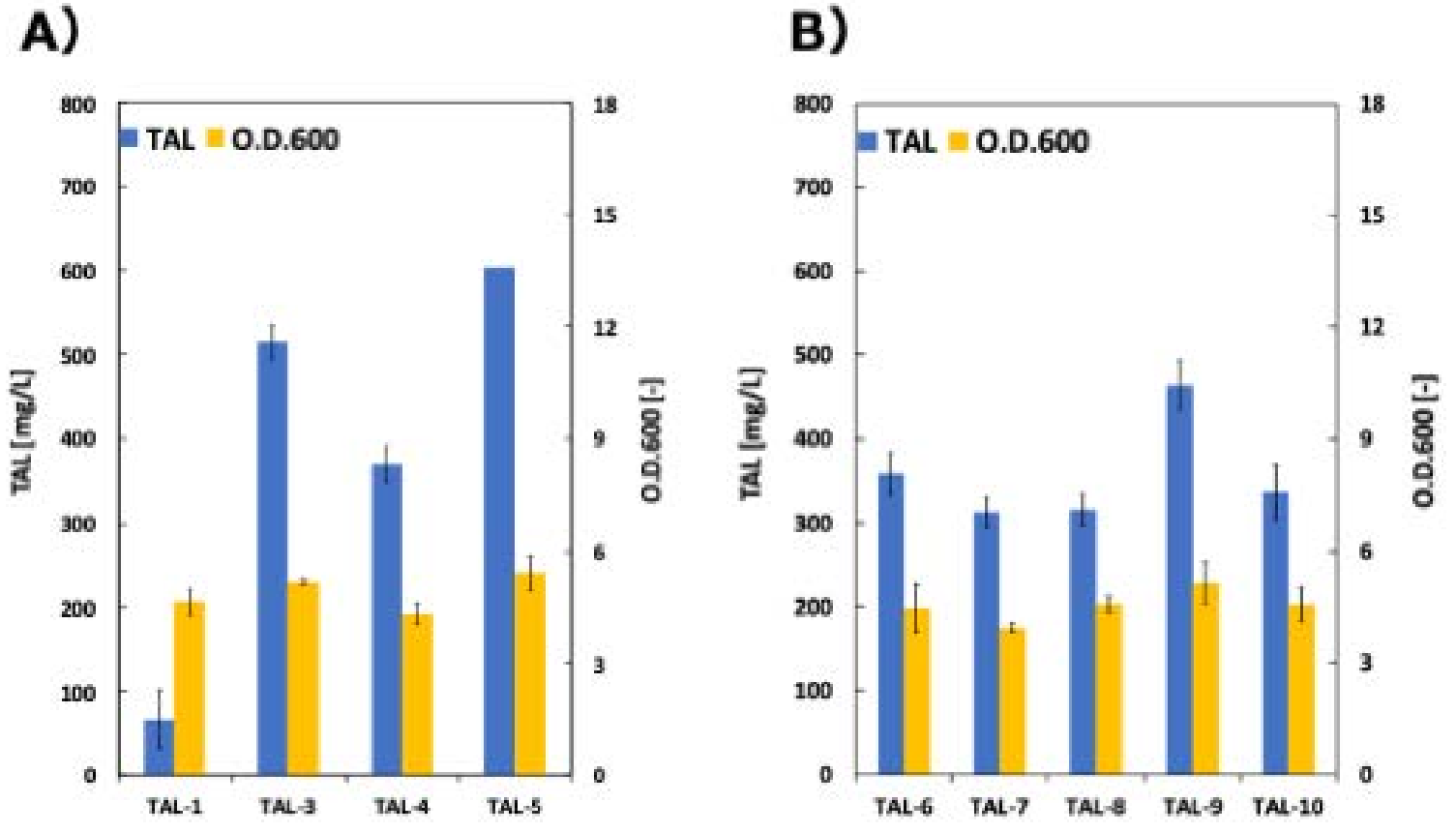
A)
TAL
O.D.600
TAL [mg/L]
O.D.600 [-]
0
100
200
300
400
500
600
700
800
0
3
6
9
12
15
18
TAL-1
TAL-3
TAL-4
TAL-5
B)
TAL
O.D.600
TAL [mg/L]
O.D.600 [-]
0
100
200
300
400
500
600
700
800
0
3
6
9
12
15
18
TAL-6
TAL-7
TAL-8
TAL-9
TAL-10

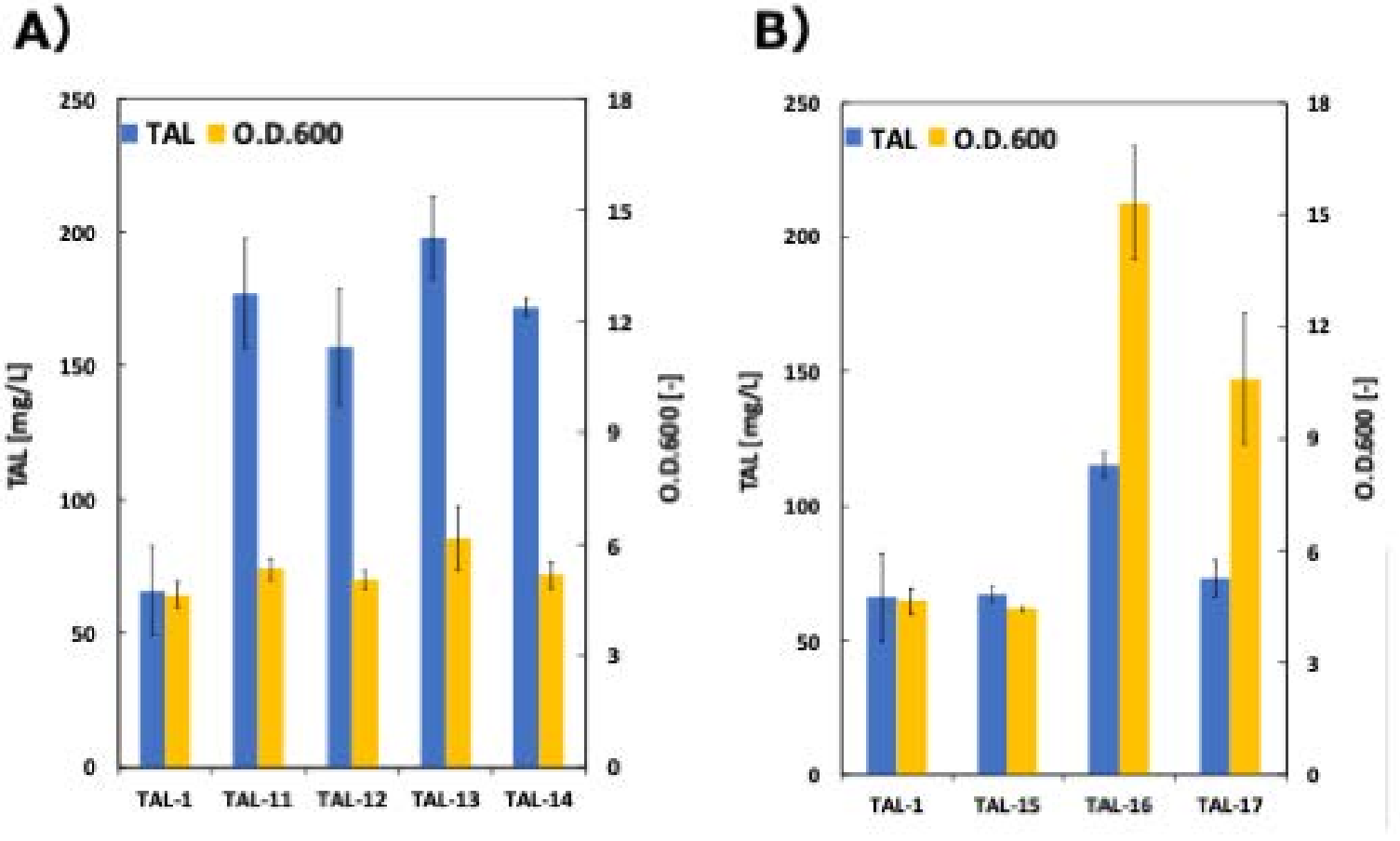
A)
TAL
O.D.600
TAL [mg/L]
O.D.600 [-]
250
200
150
100
50
0
18
15
12
9
6
3
0
TAL-1
TAL-11
TAL-12
TAL-13
TAL-14
B)
TAL
O.D.600
TAL [mg/L]
O.D.600 [-]
250
200
150
100
50
0
18
15
12
9
6
3
0
TAL-1
TAL-15
TAL-16
TAL-17

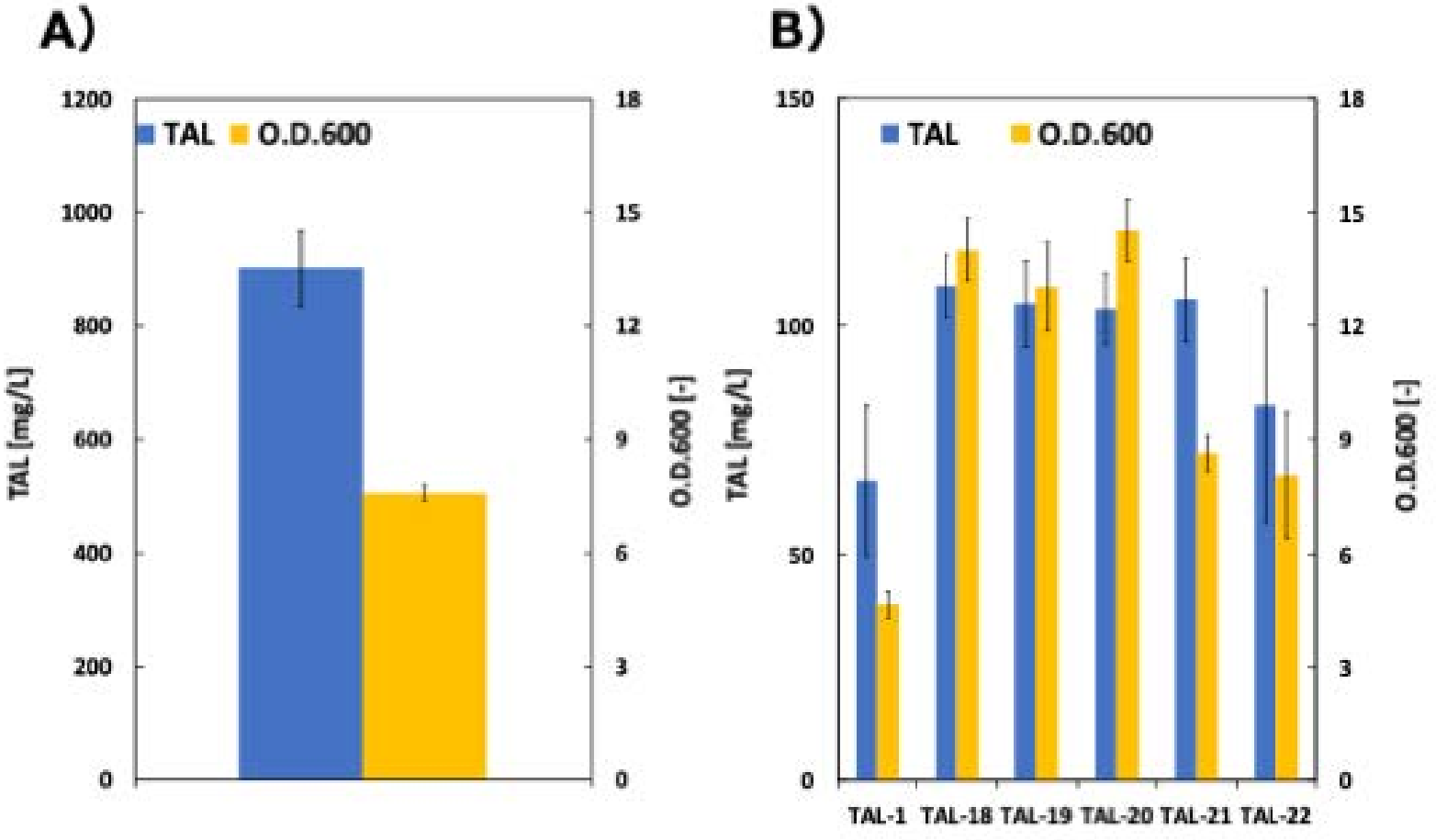
A)
TAL
O.D.600
TAL [mg/L]
O.D.600 [-]
0
200
400
600
800
1000
1200
0
3
6
9
12
15
18
B)
TAL
O.D.600
TAL [mg/L]
O.D.600 [-]
0
50
100
150
0
3
6
9
12
15
18
TAL-1
TAL-18
TAL-19
TAL-20
TAL-21
TAL-22

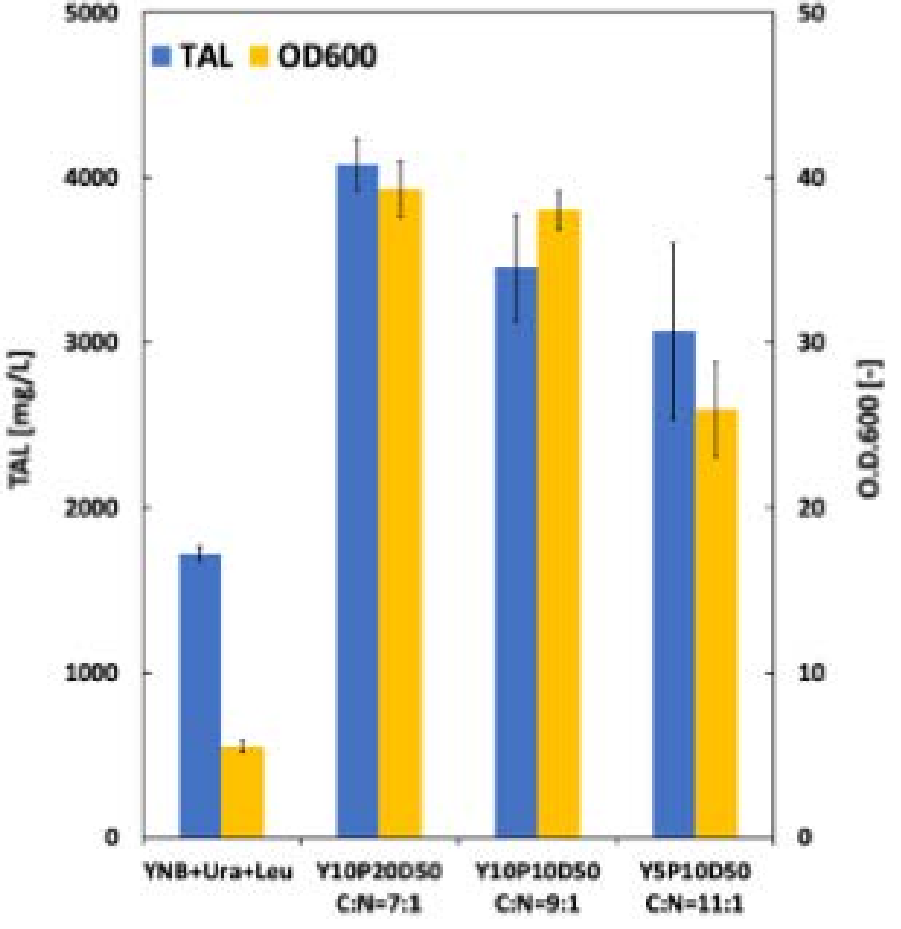
TAL
OD600
TAL [mg/L]
O.D.600 [-]
5000
4000
3000
2000
1000
0
50
40
30
20
10
0
YNB+Ura+Leu
Y10P20D50
C:N=7:1
Y10P10D50
C:N=9:1
Y5P10D50
C:N=11:1

Table 1. Strains used in this study.

Strains	**Genotype**	**Reference**
PO1f	MYA-2613	ATCC
TAL-1	*PO1f* Δ*ku70*Δ*ku80,* Δ*A08*::*2-ps*	This study
TAL-2	TAL-1, Δ*xyr11*::*2-ps*	This study
TAL-3	TAL-1, Δ*d17*::*pex10*	This study
TAL-4	TAL-1, Δ*c18*::*por1*	This study
TAL-5	TAL-1, Δ*d17*::*pex10,* Δ*c18*::*por1*	This study
TAL-6	TAL-5, Δ*inte3*::*acs1*	This study
TAL-7	TAL-5, Δ*inte3*::*pdc2*	This study
TAL-8	TAL-5, Δ*inte3*::*pdc2,* Δ*xdh*::*ald5*	This study
TAL-9	TAL-5, Δ*xyr11*::*acc1*	This study
TAL-10	TAL-5, Δ*xyr11*::*acc1,* Δ*inte3*::*acs1*	This study
TAL-11	TAL-1, Δ*cit1*	This study
TAL-12	TAL-1, Δ*cit1,* Δ*mae1,* Δ*ms1*	This study
TAL-13	TAL-1, Δ*cit1,* Δ*mae1,* Δ*ppc*	This study
TAL-14	TAL-1, Δ*cit1,* Δ*ms1,* Δ*ppc*	This study
TAL-15	TAL-1, Δ*pgi*	This study
TAL-16	TAL-1, Δ*fbp1*	This study
TAL-17	TAL-1, Δ*pgi,* Δ*fbp1*	This study
TAL-18	TAL-1, Δ*dga1*	This study
TAL-19	TAL-1, Δ*lro1*	This study
TAL-20	TAL-1, Δ*tgl3*	This study

TAL-21	TAL-1, Δ*dga1,* Δ*tgl3*	This study
TAL-22	TAL-1, Δ*dga1,* Δ*lro1,* Δ*tgl3*	This study
TAL-23	TAL-5, Δ*xyr11*::*2-ps*	This study

2

3